Electrical Engineering (2021) 103:2611–2623
https://doi.org/10.1007/s00202-021-01238-0

ORIGINAL PAPER

Maximum Torque Per Watt (MTPW) field-oriented control of induction motor

Ciro Attaianese[1] · Mauro Di Monaco[2] · Giuseppe Tomasso[2]

Received: 26 October 2020 / Accepted: 4 February 2021 / Published online: 15 March 2021

Abstract
A new field-oriented control strategy for induction motor is proposed in the paper. It is called Maximum Torque Per Watt (MTPW) and allows obtaining the minimum value of the sum of the stator and rotor losses due to joule effect, and of the iron losses, for a given value of the reference torque and of the motor speed. Iron losses have been modeled according to Steinmetz equation, separating hysteresis and eddy currents and taking into account the dependence both on the frequency and on the peak value of the flux density. Numerical and experimental results are presented to confirm the validity of the proposed approach, which allows achieving significant improvements in the efficiency of induction motor drive.

Keywords Induction motor · Field-oriented control · Maximum efficiency

Nomenclature

$\boldsymbol{i}_{\mathrm{s}}^{\mathrm{s}}$	space vector of the stator currents expressed in the stator reference frame
$\boldsymbol{i}_{\mathrm{r}}^{\prime\mathrm{s}}$	space vector of the rotor currents referred to the stator expressed in the stator reference frame
$\boldsymbol{i}_{\mathrm{mr}}^{\mathrm{s}}$	space vector of the rotor magnetizing current expressed in the stator reference frame
$i_{\mathrm{sd}}, i_{\mathrm{sq}}$	components of the stator current space vector in the rotor flux reference frame
$i'_{\mathrm{rd}}, i'_{\mathrm{rq}}$	components of the rotor current space vector referred to the stator in the rotor flux reference frame
j	unit imaginary number
p	pole pairs number
t	time
D	air gap diameter
l	active motor length
ω_{r}	motor speed
L_{m}	magnetizing inductance
$L'_{\mathrm{r}\sigma}$	rotor leakage inductance referred to the stator
R_{s}	stator resistance
R'_{r}	rotor resistance referred to the stator
T	electromagnetic torque
τ_{r}	rotor time constant
θ	rotor angle

1 Introduction

One of the "must" of classic field-oriented control of induction motor is to keep the amplitude of the rotor flux at rated value, to get a fast and accurate control of the electromagnetic torque [1,2]. However, in this way the motor efficiency can be quite poor, especially at light load conditions. The scientific literature on the optimum efficiency control of induction motor drive is wide [3–5], and the topic is currently attracting renewed interest due to the increasing focus on sustainable development issues. Many applications claim for induction motors, because of their great reliability, ruggedness, low cost, and thanks to their immunity from the potential supply difficulties of rare earth elements due to political and economic instability, which could make critical the use of PM synchronous motors. A field-oriented control strategy which

✉ Ciro Attaianese
ciro.attaianese@unina.it

Mauro Di Monaco
mauro.dimonaco@unicas.it

Giuseppe Tomasso
giuseppe.tomasso@unicas.it

[1] Dept. of Electrical Engineering and Information Technology, University of Naples "Federico II", Naples, Italy

[2] Department of Electrical and Information Engineering, University of Cassino and Southern Lazio, Cassino, Italy

guarantees the minimization of the stator current amplitude for a given load torque at steady state operating conditions is the Maximum Torque Per Ampere (MTPA) control strategy [6]. However, this strategy allows achieving the minimization only of the stator joule losses, but not of rotor joule and iron losses, which could even increase, resulting in a deterioration of motor efficiency. In [7], field-oriented control strategy has been combined with decoupled control on synchronously rotating reference frame. In [8], MTPA control strategy has been modified by introducing a torque current compensation in order to reduce the deterioration of the torque dynamic performance due to rotor flux changes. In [9], a two-stage control has been proposed, in which the control strategy is changed according to transient or steady state operations of the motor.

Several papers deal with the problem of optimizing induction motor operation even during transients. In [10], the d- and q-axis reference current components which allow minimizing transient energy losses are determined by using a dynamic programming algorithm. This control strategy is based on the offline numerical solution of Bellman's equations which requires the prior knowledge of the load torque. The results are stored as a lookup table on the controller. Other works [11–13] used Pontryagin's minimum principle for obtaining the maximum torque per current input, but also in these cases, only offline numerical solutions are given, and the control is performed by means of lookup tables.

Another mathematical approach involves the use of the calculus of variations, as shown in [14,15] and [16]. In particular, in [14] no simulation or experimental results are given, in [15], the speed is assumed constant speed during torque transients and only an approximate solution is given, while in [16], the analytical solution for extending MTPA control strategy to transient operations is given, but taking into account only stator joule losses.

In [17], a loss model controller (LMC) is proposed, which takes into account copper and iron losses with reference to the scalar control of an induction motor. In [18], an online loss minimization algorithm performs the determination of the flux level for the efficiency optimization. It is based on an induction motor loss model, which models the iron losses by means of a resistor added in parallel to the magnetizing current in the rotor flux reference frame. In this way, the dependence of iron losses on the frequency is not considered.

The contribution of this paper consists in proposing a new field-oriented control strategy for induction motor called Maximum Torque Per Watt (MTPW). It allows evaluating the reference currents for the control of the motor so as to obtain the minimum value of the sum of the stator and rotor losses due to joule effect, and of the iron losses, as a function of the reference torque and of the motor speed. Iron losses are modeled according to Steinmetz equation [19,20], separating hysteresis and eddy currents [21] and taking into account their dependence both on the frequency and on the peak value of the flux density, for every value of the speed and of the electromagnetic torque. Numerical and experimental results confirm the validity and the feasibility of the proposed control strategy. The rest of the paper is organized as follows. Section 2 presents a brief review of field-oriented and MTPA control strategies of an induction motor drive. In Sect. 3, motor losses are expressed in terms of the components of the stator and rotor currents space vectors in the rotor flux reference frame. In particular, joule losses both in stator and rotor and iron losses are taken into account. Section 4 describes the numerical and experimental validation of the proposed solution, which is compared with traditional field-oriented and MTPA control strategies. Eventually, Sect. 5 is devoted to conclusions.

2 Field-oriented vs MTPA control

Field-oriented control algorithms for induction motors are based on the assumption that the reference stator currents are instantaneously fed by means of a fast current control loop, which is performed by the power converter unit [1,2]. Thus, only the rotor equation of the mathematical model of the induction motor has to be considered, which can be expressed as:

$$\tau_r \frac{\mathrm{d}\boldsymbol{i}^{\mathrm{s}}_{\mathrm{mr}}}{\mathrm{d}t} + (1 - \mathrm{j}p\omega_{\mathrm{r}}\tau_{\mathrm{r}})\,\boldsymbol{i}^{\mathrm{s}}_{\mathrm{mr}} = \boldsymbol{i}^{\mathrm{s}}_{\mathrm{s}} \tag{1}$$

where $\boldsymbol{i}^{\mathrm{s}}_{\mathrm{s}}$ and $\boldsymbol{i}^{\mathrm{s}}_{\mathrm{mr}}$ are the space vectors of the stator and of the rotor magnetizing currents in the stator reference frame, respectively, while τ_r, p, ω_{r} have been denoted the rotor time constant, the number of pole pairs and the motor speed, respectively. The space vector of the rotor magnetizing current in the stator reference frame $\boldsymbol{i}^{\mathrm{s}}_{\mathrm{mr}}$ is defined as:

$$\boldsymbol{i}^{\mathrm{s}}_{\mathrm{mr}} = \boldsymbol{i}^{\mathrm{s}}_{\mathrm{s}} + (1 + \sigma_{\mathrm{r}})\,\boldsymbol{i}'^{\mathrm{s}}_{\mathrm{r}} \tag{2}$$

where $\boldsymbol{i}'^{\mathrm{s}}_{\mathrm{r}}$ is the space vector of the rotor current referred to the stator in the stator reference frame, and σ_{r} is the rotor leakage constant defined as:

$$\sigma_{\mathrm{r}} = \frac{L'_{\mathrm{r}\sigma}}{L_{\mathrm{m}}} \tag{3}$$

where L'_{r} and L_{m} are the rotor leakage inductance referred to the stator and the magnetizing inductance, respectively. If i_{mr} and ρ denote the absolute value and the argument of $\boldsymbol{i}^{\mathrm{s}}_{\mathrm{mr}}$, respectively, it yields

$$\boldsymbol{i}^{s}_{\mathrm{mr}} = i_{\mathrm{mr}}\ \mathrm{e}^{\mathrm{j}\rho}, \tag{4}$$

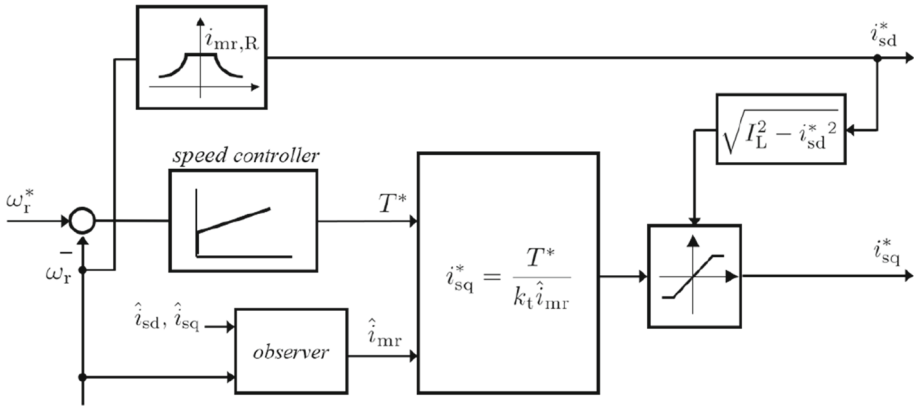

Fig. 1 Block diagram of the traditional field-oriented control strategy (T-FOC)

and then, the complex Eq. (1) can be split in real and imaginary parts:

$$\begin{cases} \tau_{\mathrm{r}} \frac{\mathrm{d}i_{\mathrm{mr}}}{\mathrm{d}t} + i_{\mathrm{mr}} = i_{\mathrm{sd}} \\ \frac{\mathrm{d}\rho}{\mathrm{d}t} = p\omega_{\mathrm{r}} + \frac{i_{\mathrm{sq}}}{\tau_{\mathrm{r}} i_{\mathrm{mr}}} \end{cases} \tag{5}$$

where i_{sd} and i_{sq} are the d- and q-axis current components of the stator current space vector in the rotor flux reference frame, which is just defined by the space vector $\boldsymbol{i}^{\mathrm{s}}_{\mathrm{mr}}$, that is

$$i_{\mathrm{sd}} + \mathrm{j}\, i_{\mathrm{sq}} = \boldsymbol{i}^{s}_{s}\ \mathrm{e}^{-\mathrm{j}\rho} \tag{6}$$

The electromagnetic torque T can be expressed as:

$$T = k_{\mathrm{t}} i_{\mathrm{mr}} i_{\mathrm{sq}} \quad \text{with} \quad k_{\mathrm{t}} = \frac{3pL_{\mathrm{m}}}{2(1+\sigma_{\mathrm{r}})} \tag{7}$$

The independence of the value of the electromagnetic torque from i_{sd} allows considering the reference value of this current component as a degree of freedom in field-oriented control strategies. Figure 1 shows the block diagram of the traditional field-oriented control (T-FOC) algorithm for an induction motor drive with speed and torque control loops. The speed controller works out the torque reference T^* on the basis of the error between reference and actual speeds, respectively, ω^*_{r} and ω_{r}. The choice of the degree of freedom i^*_{sd} is made in such a way as to achieve the maximum flux for every speed, according to a flux–speed law that keeps flux constant and equal to the rated one in the constant torque region and then hyperbolically reduces it in the constant power region, as shown in Fig. 1, where $i_{\mathrm{mr,R}}$ represents the rated values of the amplitude of the rotor magnetizing current. The value of i^*_{sq} that instantly allows guaranteeing the torque reference is determined by means of Eq. (7)

$$i^*_{\mathrm{sq}} = \frac{T^*}{k_{\mathrm{t}}\hat{i}_{\mathrm{mr}}} \tag{8}$$

where $\hat{i}_{\mathrm{mr}}$ is the amplitude of estimated space vector of the rotor magnetizing current, which is calculated by an observer or on the basis of Eq. (5) from the measurements of the mechanical speed and of stator currents. Obviously, due to motor current limitation, the value of i^*_{sq} has to be limited in order to respect the stator current constraint

$$i_{\mathrm{sd}}^2 + i_{\mathrm{sq}}^2 \le I_{\mathrm{L}}^2 \tag{9}$$

where I_{L} represents the motor current limit. Once the q-component of the stator current is eventually saturated, the T-FOC strategy provides the reference values $i^*_{\mathrm{sd}}, i^*_{\mathrm{sq}}$ of the d- and q-axis current components. The maximum torque value $T_{\mathrm{FOC,L}}$ achievable with T-FOC strategy is

$$T_{\mathrm{FOC,L}} = k_{\mathrm{t}} i_{\mathrm{mr,R}} \sqrt{I_{\mathrm{L}}^2 - i_{\mathrm{mr,R}}^2} \tag{10}$$

The choice in the T-FOC strategy of working at maximum flux in the whole operating region of the motor determines the degradation of the efficiency, which is as lower as lower is the requested value of the electromagnetic torque. To cope with this weakness of T-FOC strategy, the Maximum Torque Per Ampere (MTPA) control has been proposed in the literature [6]. This control uses the available degree of freedom represented by the choice of the value of i^*_{sd} for minimizing the amplitude of the space vector $\boldsymbol{i}^{\mathrm{s}}_{\mathrm{s}}$ for a given reference torque.

In detail, MTPA control strategy removes the constraint of keeping the rotor flux at its maximum value as in the T-FOC and calculates the reference values i^*_{sd} to get at steady state the minimum amplitude of the stator current. Because at steady state is

$$T = k_{\mathrm{t}} i_{\mathrm{sd}} i_{\mathrm{sq}} \tag{11}$$

then the value of i^*_{sd} that allows achieving this minimization is given by

$$i^*_{\mathrm{sd}} = \sqrt{\frac{T^*}{k_{\mathrm{t}}}} \tag{12}$$

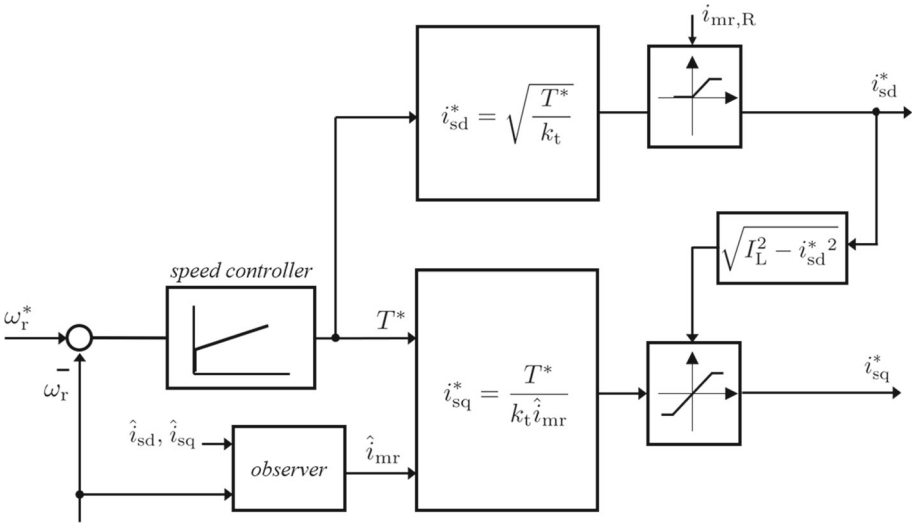

Fig. 2 Block diagram of the Maximum Torque per Ampere control strategy (MTPA)

Figure 2 shows the control diagram of the MTPA control strategy. It is possible to notice in the scheme, how the reference i^*_{sd} is determined by means of Eq. (12), whereas the i^*_{sq} is calculated on the basis of Eq. (8) for guaranteeing the instantaneous torque requested by the speed loop. At steady state, the value of i^*_{sq} satisfies the following equation in according to MTPA control strategy [6]

$$i^*_{\mathrm{sq}} = i^*_{\mathrm{sd}} = \sqrt{\frac{T^*}{k_\mathrm{t}}} \tag{13}$$

Obviously, the constraint given by the rated amplitude of the rotor magnetizing current has to be respected, and thus, a saturation block in the scheme is introduced to limit the i^*_{sd} to the value of $i_{\mathrm{mr,R}}$. Therefore, the maximum torque value $T_{\mathrm{MTPA,L}}$ achievable with MTPA strategy is given by

$$T_{\mathrm{MTPA,L}} = k_\mathrm{t} i^2_{\mathrm{mr,R}} \tag{14}$$

Considering Eq. (10), the ratio between the maximum torques achievable at steady state with T-FOC and MTPA control strategies can be expressed as

$$\beta = \frac{T_{\mathrm{MTPA,L}}}{T_{\mathrm{FOC,L}}} = \frac{\alpha}{\sqrt{1-\alpha^2}} \quad \text{with} \quad \alpha = \frac{i_{\mathrm{mr,R}}}{I_\mathrm{L}} \tag{15}$$

Thus, if the MTPA control strategy is adopted, for avoiding a motor derating, the control strategy has to be switched from MTPA to T-FOC when $T^* > T_{\mathrm{MTPA,L}}$.

In this way, at steady state with the MTPA control strategy the minimum of the stator joule losses is achieved for each value of the electromagnetic torque $T^* \leq T_{\mathrm{MTPA,L}}$. However, this does not imply that the overall losses of the motor are the minimum. Minimizing the overall motor losses is precisely the goal of the proposed Maximum Torque Per Watt (MTPW) control strategy, which is described below. It uses the available degree of freedom to determine the reference value i^*_{sd} to minimize the motor total losses for every value of the electromagnetic torque at steady state, taking into account the joule losses and the iron losses as well.

3 Motor losses in field-oriented coordinates

As explained in Sect. (2), the goal of the proposed MTPW control strategy is the minimization at steady state of the total losses of the motor, exploiting the degree of the freedom given by the value of i^*_{sd} to be imposed. Thus, in this section, the mathematical model of the motor losses used for the development of the MTPW control strategy is presented. In detail, the expressions of the joule losses, both in stator and rotor, and of the iron losses are given in terms of current components expressed in the rotor flux reference frame.

3.1 Stator joule losses

If space vectors are defined in the classical non-power invariant form, for the generic phase quantity a_k the space vector $\boldsymbol{a}$ is defined as

$$\boldsymbol{a} = \frac{2}{3}\sum_{k=1}^{3} a_\mathrm{k} \tag{16}$$

Therefore, the instantaneous stator joule losses p_{js} are

$$p_{\mathrm{js}} = \frac{3}{2} R_\mathrm{s}\left(i^2_{\mathrm{sd}} + i^2_{\mathrm{sq}}\right) \tag{17}$$

where R_s is the stator resistance.

3.2 Rotor joule losses

The instantaneous rotor joule losses p_{jr} can be expressed as

$$p_{\mathrm{jr}} = \frac{3}{2} R'_{\mathrm{r}} \left(i'^{2}_{\mathrm{rd}} + i'^{2}_{\mathrm{rq}} \right) \tag{18}$$

where R'_{r} is the rotor resistance referred to the stator, and i'_{rd} and i'_{rq} represent the d- and q-axis components of the space vector of the rotor current, referred to the stator, in the rotor flux reference frame, which are given by

$$i'_{\mathrm{rd}} + \mathrm{j}\, i'_{\mathrm{rq}} = \boldsymbol{i}'^{\,\mathrm{s}}_{\mathrm{r}}\, \mathrm{e}^{-\mathrm{j}\rho} \tag{19}$$

Therefore, Eq. (2) yields

$$\begin{cases} i_{\mathrm{mr}} = i_{\mathrm{sd}} + (1+\sigma_r) i'_{\mathrm{rd}} \\ 0 \quad\; = i_{\mathrm{sq}} + (1+\sigma_r) i'_{\mathrm{rq}} \end{cases} \tag{20}$$

Since i_{mr} is equal to i_{sd} at the steady state, this leads $i'_{\mathrm{rd}} = 0$. Thus, p_{jr} can be expressed as a function of the q-axis component of the stator current space vector

$$p_{\mathrm{jr}} = \frac{3}{2} \frac{R'_{\mathrm{r}}}{(1+\sigma_{\mathrm{r}})^2}\, i^2_{\mathrm{sq}} \tag{21}$$

3.3 Iron losses

The steady state iron losses p_{Fe} can be evaluated according to the Steinmetz equation [19,20] separating the iron losses [21] into static hysteresis losses p_{hyst}, and dynamic eddy currents p_{ec}, that is

$$p_{\mathrm{Fe}} = p_{\mathrm{hyst}} + p_{\mathrm{ec}} = C_{\mathrm{hyst}} f B^2_M + C_{\mathrm{ec}} f^2 B^2_M \tag{22}$$

where B_M is the peak value of the flux density and f the frequency, and where C_{hyst} and C_{ec} are the hysteresis and the eddy current loss coefficients, respectively. Because the space vector of the rotor flux $\boldsymbol{\phi}^s_{\mathrm{r}}$ in the stator reference frame is given by

$$\boldsymbol{\phi}^s_{\mathrm{r}} = L_{\mathrm{m}} \boldsymbol{i}^s_{\mathrm{mr}} = L_{\mathrm{m}} i_{\mathrm{mr}}\, \mathrm{e}^{\mathrm{j}\rho}, \tag{23}$$

it yields

$$f \simeq \frac{\mathrm{d}\rho}{\mathrm{d}t} \tag{24}$$

and if a sinusoidal air gap flux density is assumed, with an approximation that is so much better the smaller is σ_{r}, it turns out

$$B_M \simeq \frac{p}{Dl} |\boldsymbol{\phi}^s_{\mathrm{r}}| = \frac{pL_{\mathrm{m}}}{Dl} i_{\mathrm{mr}} \tag{25}$$

where D and l are the air gap diameter and the active length of the motor, respectively.
Therefore, iron losses can be expressed as

$$p_{\mathrm{Fe}} = k_1 \frac{\mathrm{d}\rho}{\mathrm{d}t}\, i^2_{\mathrm{mr}} + k_2 \left(\frac{\mathrm{d}\rho}{\mathrm{d}t} \right)^2 i^2_{\mathrm{mr}} \tag{26}$$

with

$$k_1 = C_{\mathrm{hyst}} \left(\frac{pL_{\mathrm{m}}}{Dl} \right)^2 \qquad k_2 = C_{\mathrm{ec}} \left(\frac{pL_{\mathrm{m}}}{Dl} \right)^2 \tag{27}$$

The determination of the coefficients C_{hyst} and C_{ec} can be performed according to [21–23], and requires the knowledge of the data sheet of the magnetic laminations constituting the stator and the rotor of the motor. Experimental corrections [24–27] can be introduced to take into account the increase due to PWM inverter supply.
From the second equation of the set of Eq. (5), taking into account that at the steady state i_{mr} is equal to i_{sd}, it yields

$$p_{\mathrm{Fe}} = \left[k_1 \left(p\omega_{\mathrm{r}} + \frac{i_{\mathrm{sq}}}{\tau_{\mathrm{r}} i_{\mathrm{sd}}} \right) + k_2 \left(p\omega_{\mathrm{r}} + \frac{i_{\mathrm{sq}}}{\tau_{\mathrm{r}} i_{\mathrm{sd}}} \right)^2 \right] i^2_{\mathrm{mr}} \tag{28}$$

4 The MTPW control strategy

From the foregoing section, it is immediate to derive the expression of the sum p_{tot} of joule and iron losses as a function of i_{sq}, T^*, and of motor parameters

$$p_{\mathrm{tot}} = p_{\mathrm{js}} + p_{\mathrm{jr}} + p_{\mathrm{Fe}} = \frac{A i^4_{\mathrm{sq}} + B i^2_{\mathrm{sq}} + C}{i^4_{\mathrm{sq}}} \tag{29}$$

with

$$A = \frac{3}{2} \left[R_{\mathrm{s}} + \frac{R'_{\mathrm{r}}}{(1+\sigma_{\mathrm{r}})^2} \right] + \frac{k_2}{\tau^2_{\mathrm{r}}} \tag{30}$$

$$B = \frac{T^*}{k_{\mathrm{t}}} \frac{(1 + 2k_2 p\omega_{\mathrm{r}})}{\tau_{\mathrm{r}}} \tag{31}$$

$$C = \frac{3}{2} \frac{T^*}{k_{\mathrm{t}}} (R_{\mathrm{s}} + k_1 p\omega_{\mathrm{r}} + k_2 p^2 \omega^2_{\mathrm{r}}) \tag{32}$$

For a given value of T^*, the minimum value of the function $p_{\mathrm{tot}}(i_{\mathrm{sq}})$ is achieved when

$$i_{\mathrm{sq}} = \sqrt[4]{\frac{C}{A}} = \gamma \sqrt{\frac{T^*}{k_{\mathrm{t}}}} \tag{33}$$

with

$$\gamma = \left\{ \frac{\frac{3}{2}R_s + k_1 p \omega_r + k_2 p^2 \omega_r^2}{\frac{3}{2}\left[R_s + \frac{R'_r}{(1+\sigma_r)^2}\right] + \frac{k_2}{\tau_r^2}} \right\}^{1/4} \tag{34}$$

Since i_{mr} is equal to i_{sd} at the steady state, the value of i_{sd}^* that allows minimizing the total losses of the induction motor drive for a given value of the reference torque is obtained by substituting Eq. (33) into Eq. (7)

$$i_{sd}^* = \frac{1}{\gamma}\sqrt{\frac{T^*}{k_t}} \tag{35}$$

As difference with the two previous control strategies, T-FOC and MTPA, in the proposed MTPW control strategy i_{sd}^* is a function of the reference torque and of the mechanical speed, being γ a function of ω_r, according to Eq. (34).
The block diagram of the proposed MTPW control strategy is shown in Fig. 3. The adoption of i_{sd}^* in according to Eq. (35) minimizes the total power losses. To guarantee the respect of the requested torque imposed by the speed controller, the i_{sq}^* is calculated by means of the instantaneous expression of the electromagnetic torque given by Eq. (8). Obviously, at the steady state, i.e., $i_{mr} = i_{sd}^*$, Eq. (33) has to be satisfied and, thus, i_{sq}^* is given by

$$i_{sq}^* = \gamma\sqrt{\frac{T^*}{k_t}} = \gamma^2 i_{sd}^* \tag{36}$$

The proposed MTPW control strategy does not require at the steady state that $i_{sq}^* = i_{sd}^*$ as in the MTPA control strategy, but in order to minimize the total power losses i_{sq}^* is a function of i_{sd}^* and γ, which in turn is a function of the motor parameters and of the speed ω_r. The two control strategies have the same performance just in one operating point that is achieved when $\gamma = 1$.
As for T-FOC and MTPA control strategies, the maximum torque value achievable by means of the MTPW control strategy, $T_{MTPW,L}$, has to be defined. In detail, $T_{MTPW,L}$ is obtained taking into account the respect of two current constraints: the rated amplitude of the rotor magnetizing current $i_{mr,R}$ and the motor current limit I_L. Considering these constraints, two torque limit values can be defined T_{MTPW,L_1} and T_{MTPW,L_2}. The first one represents the torque limit as a function of $i_{mr,R}$, and the second one gives the torque limit as a function of I_L. The expressions of the two torque limits are

$$\begin{cases} T_{MTPW,L_1} = k_t \gamma^2 i_{mr,R}^2 \\ T_{MTPW,L_2} = k_t \gamma^2 \dfrac{{I_L}^2}{1+\gamma^4} \end{cases} \tag{37}$$

Because for each speed value the two torque limits have to be always respected, it is

$$T_{MTPW,L} = min\{T_{MTPW,L_1}(i_{mr,R}), T_{MTPW,L_2}(I_L)\} \tag{38}$$

Denoting with γ_L the value of γ for which the functions T_{MTPW,L_1} and T_{MTPW,L_2} are equal, the expression of the $T_{MTPW,L}$ is given by

$$\begin{cases} \gamma \le \gamma_L & T_{MTPW,L} = k_t \gamma^2 i_{mr,R}^2 \\ \gamma > \gamma_L & T_{MTPW,L} = k_t \gamma^2 \dfrac{{I_L}^2}{1+\gamma^4} \end{cases} \tag{39}$$

with

$$\gamma_L = \left(\frac{{I_L}^2 - {i_{mr,R}}^2}{{i_{mr,R}}^2}\right)^{1/4} \tag{40}$$

Thus, from Eq. (10) it yields

$$\begin{cases} \gamma \le \gamma_L & \delta = \dfrac{T_{MTPW,L}}{T_{FOC,L}} = \gamma^2 \dfrac{\alpha}{\sqrt{1-\alpha^2}} \\ \gamma > \gamma_L & \delta = \dfrac{T_{MTPW,L}}{T_{FOC,L}} = \dfrac{\gamma^2}{(1+\gamma^4)\sqrt{1-\alpha^2}} \end{cases} \tag{41}$$

Obviously, for avoiding the motor derating, a switch between MTPW, MTPA and T-FOC control strategies has to be made, according to the values of the reference torque T^* and of the torque limits achievable with each control strategy. Since γ is a function of the mechanical speed, the choice of the control strategy depends both on T^* and γ as shown in Fig. (4), in which the flowchart of the proposed field-oriented control strategy is represented. In particular, for each value of the mechanical speed

- when $\gamma \le \gamma_L$:
  - if $\gamma \le 1$, the control strategy has to be switched first from MTPW to MTPA for $T_{MTPW,L} < T^* \le T_{MTPA,L}$, and then, from MPTA to T-FOC for $T^* > T_{MTPA,L}$;
  - if $1 < \gamma \le \gamma_L$, the control strategy has to be switched from MTPW to T-FOC for $T^* > T_{MTPW,L}$;
- when $\gamma > \gamma_L$:
  - the control strategy has to be switched from MTPW to T-FOC for $T^* > T_{MTPW,L}$.

5 Numerical and Experimental Analysis

The performances of the proposed MTPW field-oriented control algorithm have been validated and compared with the

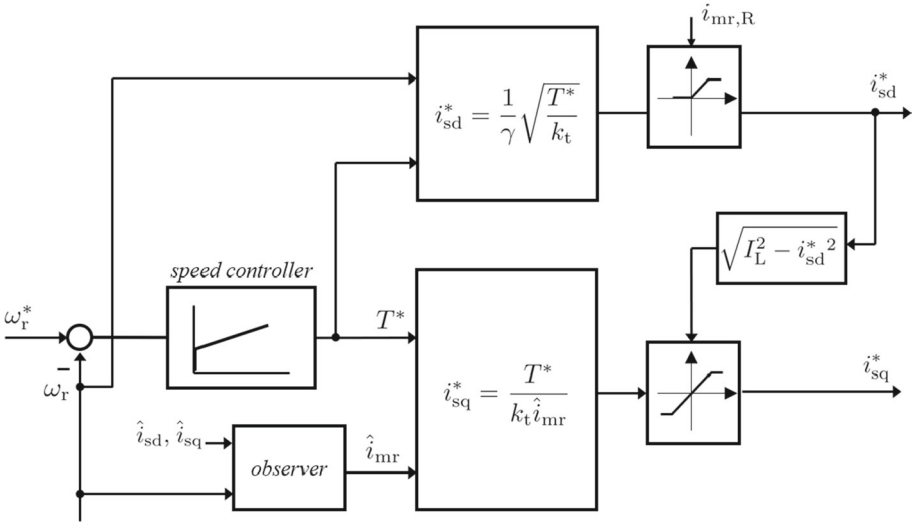

Fig. 3 Block diagram of the proposed Maximum Torque Per Watt strategy (MTPW)

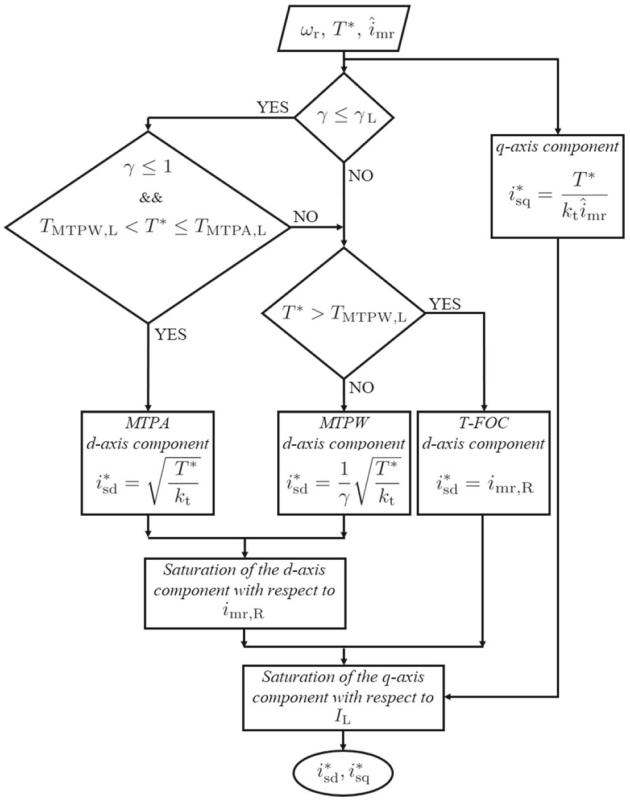

Fig. 4 Evaluation of i^*_{sd}, i^*_{sq} for the proposed field-oriented control strategy

Table 1 Main data of the tested motor and of the control system

Induction Motor		
Rated power	1.1	kW
Rated torque	7.48	Nm
Rated voltage (rms)	380	V
Rated current (rms)	2.6	A
Rated motor speed	150	rad/s
Pole pairs	2	
Stator resistance	7.5	mΩ
Rotor resistance referred to stator	4.8	mΩ
Stator leakage inductance	20	mH
Rotor leakage inductance	20	mH
Air gap inductance	430	mH
Efficiency	0.7	
k_1	$6.5 \cdot 10^{-2}$	VsA^{-1}
k_2	$2.1 \cdot 10^{-4}$	Vs^2A^{-1}
Control System		
Processor frequency of the DS1006 board	2.8	GHz
Maximum frequency of the DS3002 encoder board	750	kHz
Resolution of the DS2004 A/D Board	16	bit
Switching frequency	5	kHz

ones of T-FOC and MTPA controls through several simulation and experimental tests. The numerical model of the induction motor drive has been developed in MATLAB-Simulink® environment using the same parameters of the real components of the experimental setup (Table 1) in order to compare the numerical and experimental results as well. For the sake of clarity, in the following figures related to analysis results, each of the three above considered control strategies has been uniquely associated with a color:

- FOC—red
- MTPA—green
- MTPW—blue

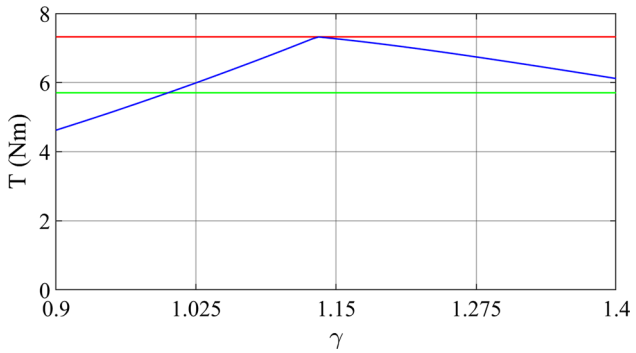

Fig. 5 Maximum torque in steady state for T-FOC (red), MTPA (green) and MTPW (blue) control strategies

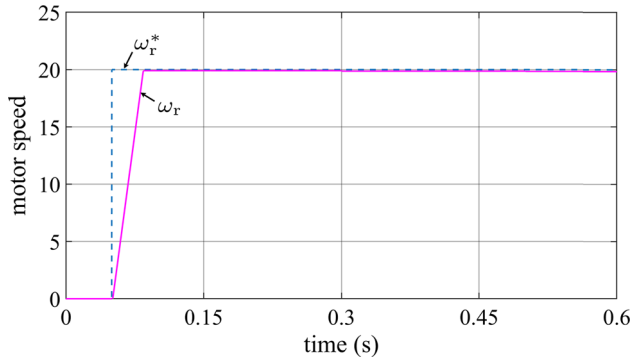

Fig. 6 Comparison between the actual motor speed and the reference one, equal to 20 rad/s, when the load torque profile in Fig. 7 is imposed

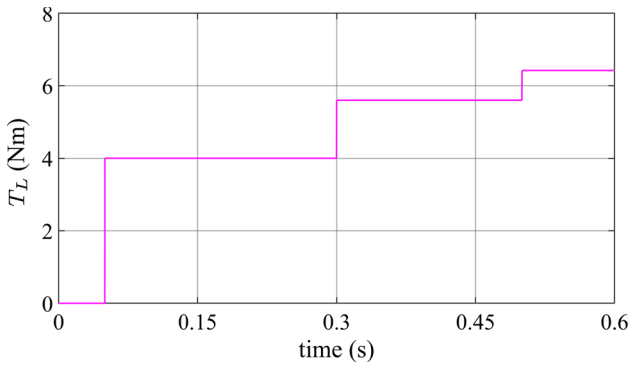

Fig. 7 Imposed profile of the load torque

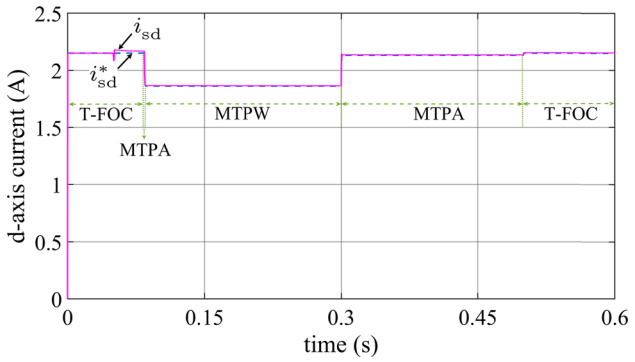

Fig. 8 Comparison between i_{sd}^* and i_{sd}^* during the load torque variation in Fig. 7, which requires the adoption of the all three control strategies T-FOC, MTPA and MTPW to guarantee the control of the motor speed at 20 rad/s

At the beginning, the constant torque domains have been studied for T-FOC, MTPA and MTPW control strategies on the basis of Eqs. (10), (14) and (39), respectively. Figure (5) shows the torque limits as a function of γ, and thus of mechanical speed, for the three field-oriented control strategies in the case of the considered motor. As presented in sections (2) and (4), the MTPA and the proposed MTPW control strategies do not allow covering the entire torque domain of the T-FOC control strategy, which is represented by the constant value 7.3 Nm that is equal to the rated torque of the motor, T_R. Moreover, when γ is lower than 1, the torque limit of MTPW control is lower than one of the MTPA controls, whereas the torque limit of MTPW is higher than the MTPA one for values of $\gamma > 1$.

Closed-loop speed control of the induction motor drive with a torque load variation has been taken into account in order to verify the dynamic performance of the proposed field-oriented control strategy, which is described by the flowchart in Fig. (4). To analyze the switch between MTPW, MTPA and T-FOC control strategies, a reference motor speed, ω_r^*, equal to 20 rad/s has been imposed as shown in Fig. (6). The value of γ at 20 rad/s is equal to 0.89 which is lower than 1. Thus, imposing the load torque profile of Fig. (7), which is characterized by different values that exceed the torque limits at 20 rad/s of MTPA and MTPW, the proposed field-oriented control strategy has to switch between the three strategies to guarantee the control of the motor speed at 20 rad/s and the respect of the torque demand. Figure (8) shows how the three strategies are selected during the considered load torque variation test and how i_{sd}^* accordingly varies. It is possible to notice that at the beginning, when the required motor torque is high for accelerating up to the reference speed, the T-FOC strategy is selected from $t = 0.0s$ to $t = 0.08421s$. At $t = 0.08428s$, the MPTW strategy is selected because the torque load at the steady state is equal to 4.0 Nm, which is below the MTPW torque limit that is 5.34 Nm. Obviously, to move from T-FOC to MPTW, the proposed control adopts the MTPA strategy during the reduction transient of the motor torque, for $0.08421s \leq t \leq 0.08428s$. At $t = 0.3s$, the load torque increases and its new value equal to 5.6 Nm is higher than the MTPW torque limit and lower than the MTPA one equal to 5.70 Nm. Thus, in the new load condition, the proposed control selects the MTPA strategy. At $t = 0.5s$, the torque load reaches 6.42 Nm exceeding the MTPA torque limit and, thus, the T-FOC strategy is again adopted. The i_{sq}^* that instantly allows guaranteeing the motor torque reference is reported in Fig. (9). Thanks to a correct tracking of the i_{sd}^*

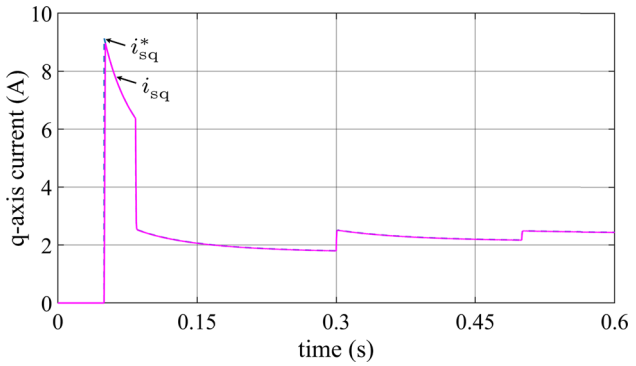

Fig. 9 Comparison between i^*_{sq} and i^*_{sq} during the load torque variation in Fig. 7

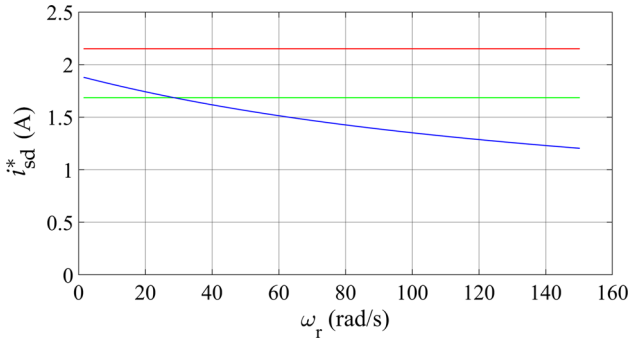

Fig. 10 Reference value of the d-axis current component i^*_{sd} for T-FOC (red), MTPA (green) and MTPW (blue) control strategies when load torque T_L=3.5 Nm and $0 \leq \omega_r \leq \omega_{r,R}$

and i^*_{sq} by d- and q-axis current components of the motor, as shown in Figs. (8) and (9), the proposed field-oriented control strategy allows controlling the motor speed under load torque variation. To fully compare the performance of the three control strategies in terms of the total power losses and of their distribution, a value of the reference torque T^*=3.5 Nm has been considered. In fact, this value of T^* can be satisfied with all the field-oriented control strategies. Figure (10) shows how the three techniques select the degree of the freedom i^*_{sd} within the range speed $0 \leq \omega_r \leq \omega_{r,R}$, where $\omega_{r,R}$ is the rated mechanical speed of the motor. In the analysis, a constant step size of 1.5 rad/s has been used for the mechanical speed. It is possible to notice that i^*_{sd} is constant for T-FOC and MTPA control strategies within the whole speed interval. In fact, as described in Sect. 2, in the case of the T-FOC control strategy, it is equal to $i_{mr,R}$ for every value of speed below to the rated one. In MTPA control strategy, the value of i^*_{sd} is constant because it is calculated according to Eq. (12), where i^*_{sd} is just a function of T^* and not of ω_r. Instead, in the case of the proposed MTPW control strategy, i^*_{sd} varies with the ω_r according to Eq. (35), where γ is a function of the ω_r.

Figure (11) shows the comparison of the amplitude of the stator current space vector at the steady state for every value

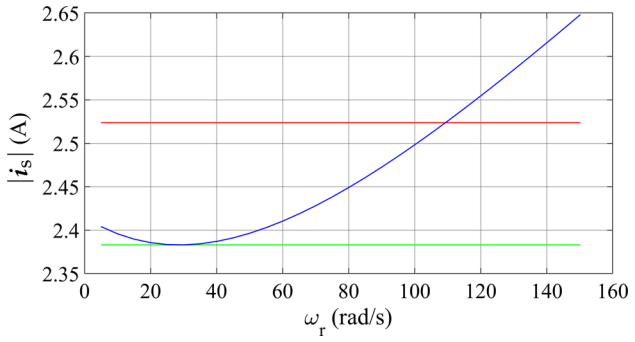

Fig. 11 Comparison of the amplitude of the stator current, $|i_s|$, in steady state, for T-FOC (red), MTPA (green) and MTPW (blue) control strategies when load torque T_L=3.5 Nm and ω_r $0 \leq \omega_r \leq \omega_{r,R}$

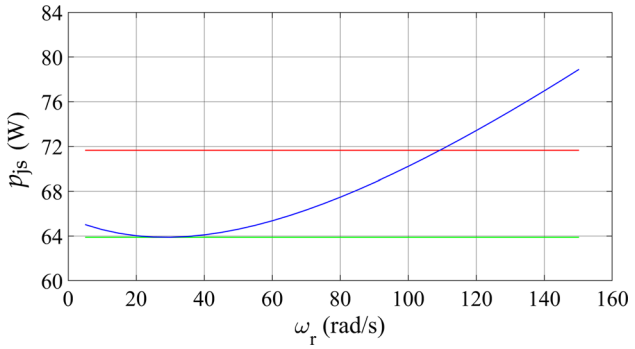

Fig. 12 Comparison of the stator joule losses, p_{js}, in steady state, for T-FOC (red), MTPA (green) and MTPW (blue) control strategies when load torque T_L=3.5 Nm and $0 \leq \omega_r \leq \omega_{r,R}$

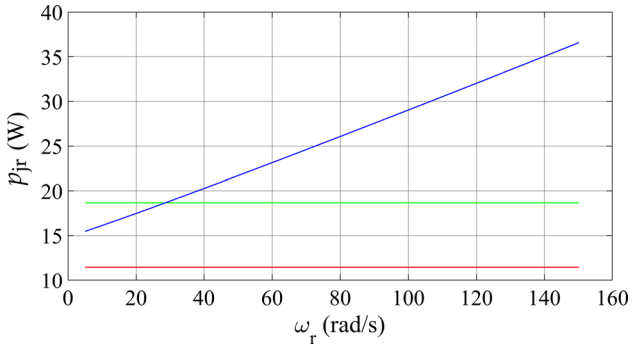

Fig. 13 Comparison of the rotor joule losses, p_{jr}, in steady state, for T-FOC (red), MTPA (green) and MTPW (blue) control strategies when load torque T_L=3.5 Nm and $0 \leq \omega_r \leq \omega_{r,R}$

of the ω_r interval for the three control strategies, when a load torque T_L equal to 3.5 Nm is imposed. The MTPA control strategy minimizes the amplitude of the stator currents with respect to the other two control strategies. This allows achieving the minimum stator joule losses at the steady state for the MTPA solution as shown in Fig. (12). With reference to the rotor joule losses shown in Fig. (13), the T-FOC control strategy allows achieving minimum values of these losses at the steady state operating conditions. The proposed MTPW

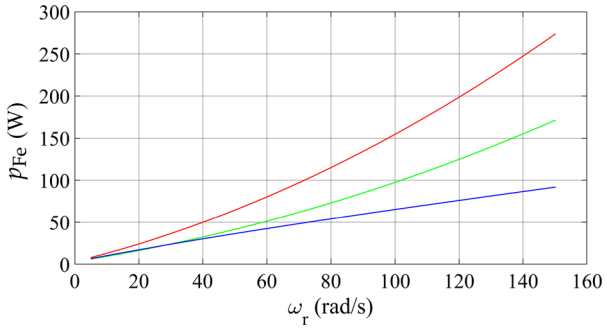

Fig. 14 Comparison of the iron power losses, p_{Fe}, in steady state, for T-FOC (red), MTPA (green) and MTPW (blue) control strategies when load torque T_L=3.5 Nm and $0 \leq \omega_r \leq \omega_{r,R}$

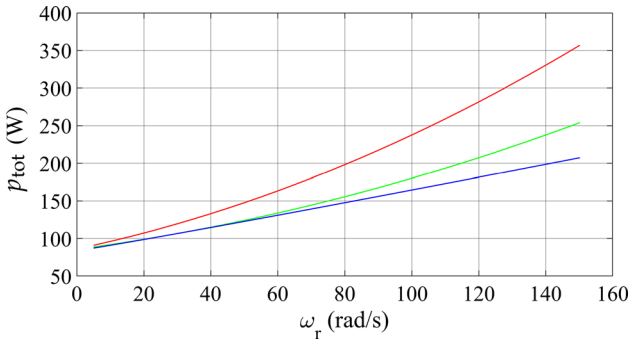

Fig. 15 Comparison of the total power losses, p_{tot}, in steady state, for T-FOC (red), MTPA (green), and MTPW (blue) control strategies when load torque T_L=3.5 Nm and $0 \leq \omega_r \leq \omega_{r,R}$

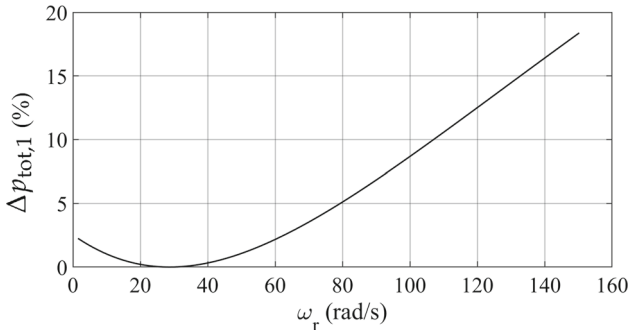

Fig. 16 Reduction of the total power losses, $\Delta p_{tot,1}$, obtained by the proposed MTPW control strategy with respect of the MTPA one when $T_l = 3.5$ Nm and $0 \leq \omega_r \leq \omega_{r,R}$

control strategy has lower rotor joule losses than MTPA control strategy for $\gamma < 1$, while MTPW rotor losses are higher than the MTPA ones when $\gamma > 1$. Figure (14) shows how the proposed MTPW control strategy allows achieving minimum values of the iron power losses in comparison with the T-FOC and MTPA control strategies within the entire speed interval. In terms of the total power losses, given by Eq. (29), the proposed MTPW control strategy allows minimizing their values as shown in Fig. (15), considering the same operating conditions of the induction motor drive at

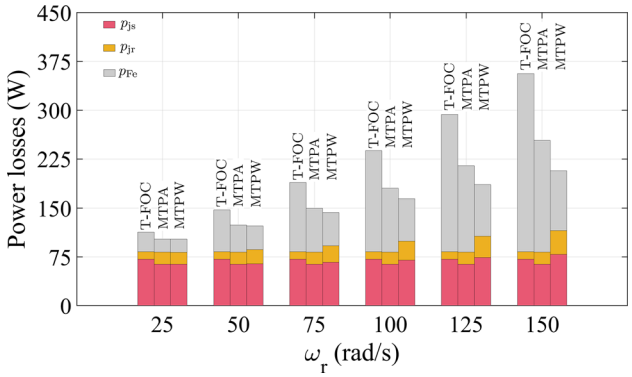

Fig. 17 Comparison of the power losses distribution at steady state, for T-FOC, MTPA and MTPW control strategies when load torque T_L=3.5 Nm and $0 \leq \omega_r \leq \omega_{r,R}$

the steady state for the three control strategies. Figure (16) shows the MTPW total losses reduction with respect to the MPTA ones in percentage, $\Delta p_{tot,1}$, that is calculated as:

$$\Delta p_{tot,1} = 100 \left| \frac{p_{tot,MTPW} - p_{tot,MTPA}}{p_{tot,MTPA}} \right| \tag{42}$$

where $p_{tot,MTPW}$ and $p_{tot,MTPA}$ are the total power losses of the induction motor when MTPW and MTPA control strategies are adopted, respectively. For ω_r=28.7 rad/s, to which γ=1 corresponds, the total losses of the two control strategies are identical. In fact, at the operating point T_L=3.5 Nm and ω_r=28.7 rad/s, the values of i_{sd}^* and i_{sq}^* for MTPA (Eq.(13)) and MTPW (Eq. (36)) control strategies are equal. The highest value of the total losses reduction, 18.4 %, has been achieved by means of the proposed MTPW control strategy at the maximum speed considered in the analysis, which is equal to rated mechanical speed. Figure 17 shows the power losses distribution at steady state of the three control strategies: T-FOC, MTPA and MTPW, when load torque T_L=3.5 Nm and $0 \leq \omega_r \leq \omega_{r,R}$.

Once verified that the proposed MTPW control strategy allows minimizing the power losses for a particular value of the electromagnetic torque equal to 3.5 Nm for the entire speed range, the performance comparison has been extended by varying the value of the electromagnetic torque from 0 up to T_R, with a constant step size equal to 0.1 Nm. Obviously, the comparison takes into account the torque limits at the steady state of the three control strategies in Fig. (3). Thus, the total power losses of the proposed MTPW control strategy have been first compared with the ones of MTPA control strategy until both the field-oriented controls are applicable, i.e., T^* is lower than $T_{MTPA,L}$ that is equal to 5.7 Nm. Figure (18) shows the results of this comparison by means of a 3D graph with torque on x-axis, speed on y-axis and the reduction of the total power losses $\Delta p_{tot,1}$ on the z-axis.

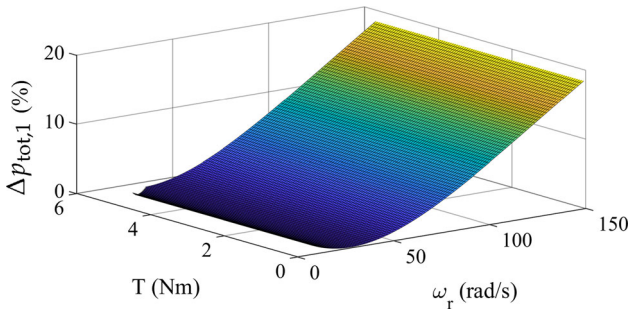

Fig. 18 Reduction of the total power losses, $\Delta p_{\text{tot},1}$, obtained by the proposed MTPW control strategy with respect of the MTPA control strategy when $0 \leq T_l \leq T_{\text{MTPA,L}}$ and $0 \leq \omega_r \leq \omega_{r,R}$

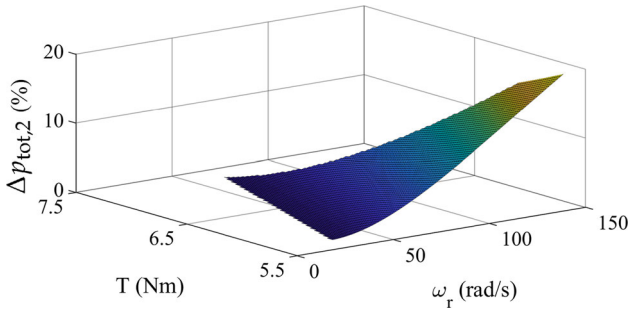

Fig. 19 Reduction of the total power losses, $\Delta p_{\text{tot},2}$, obtained by the proposed MTPW control strategy with respect of the T-FOC control strategy when $T_l > T_{\text{MTPA,L}}$ and $0 \leq \omega_r \leq \omega_{r,R}$

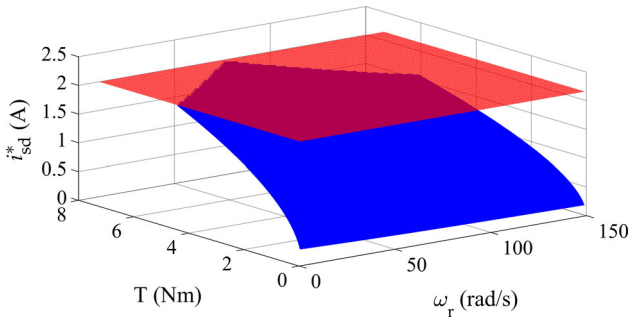

Fig. 20 Reference value of the d-axis current component i_{sd}^* for the MTPW control strategy (blue) with respect to the constraint of the maximum value of i_{sd} (red) within of the whole control domain

When the MTPA control strategy cannot be adopted, i.e., $T^* > T_{\text{MTPA,L}}$, total power losses of the proposed MTPW control strategy have been compared with the ones of the T-FOC control strategy. As for the previous comparison, the results are reported in a 3D graph in Fig. (19) with torque on x-axis, speed on y-axis and the reduction of the total power losses $\Delta p_{\text{tot},2}$ on the z-axis, which is defined as:

$$\Delta p_{\text{tot},2} = 100 \left| \frac{p_{\text{tot,MTPW}} - p_{\text{tot,T-FOC}}}{p_{\text{tot,T-FOC}}} \right| \tag{43}$$

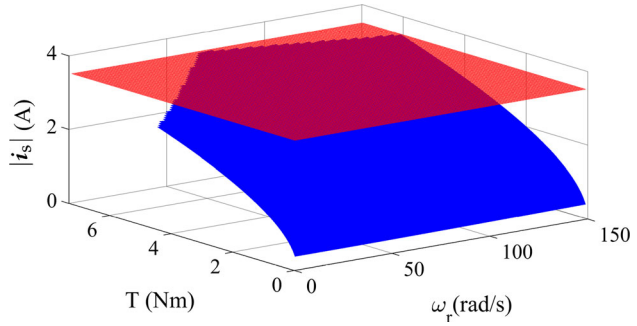

Fig. 21 Amplitude of the stator currents space vector, $|i_s|$, for the MTPW control strategy (blue) with respect to the constraint of the maximum allowable value (red) in steady state

where $p_{\text{tot,T-FOC}}$ denotes the total power losses of the induction motor when T-FOC is adopted. The proposed MTPW control strategy allows achieving a reduction of total power losses with respect to the other two T-FOC and MTPA control strategies in all the steady state operating conditions, when it is applicable. With reference to Fig. (18), MTPW control algorithm has the same power losses of the MTPA one when the mechanical speed is equal to 28.7 rad/s, because γ is equal to 1 for this value of ω_r. In all other working points where MTPW technique can be used, it allows obtaining a reduction of the total power losses, $\Delta p_{\text{tot},1}$, that increases with the growth of the values of the torque and of the mechanical speed, confirming the maximum percentage value of the power losses reduction equal to 18.4%. The proposed MTPW control strategy allows achieving a reduction of the total power losses with respect to T-FOC control strategy technique as shown in Fig. (19) as well. The higher total power losses reduction $\Delta p_{\text{tot},2}$ is obtained in correspondence of lower torques and higher mechanical speeds. The maximum value of $\Delta p_{\text{tot},2}$ is equal to 18.4%, and it is achieved for the operating point with T_L=5.7 Nm and ω_r=$\omega_{r,R}$. Figures (20) and (21) show the imposition of the set of equations (39) and (40) allows respecting the rated values of the magnetizing current and of the limit current, red surfaces, for the entire constant torque region of the MTPW field-oriented control algorithm.

With reference to the picture of the experimental setup, as shown in Fig. (22), the motor is fed by a standard VSI converter based on Mitsubishi PM100DSA120 IPMs. The different control strategies have been implemented by means of DS1006 processor board of a dSPACE® modular system. It has been interfaced with symmetrical SVM unit based on Altera® CPL EPM7160SLC8410. The modulation unit generates the synchronization signal, with a period of 200μs, which is used to run the processor interrupt control task. In detail, within each sampling time T_s, the control unit works out the modulation pattern to be imposed for inverter modulation in the next T_s by DS4003 digital I/O board. DS3002

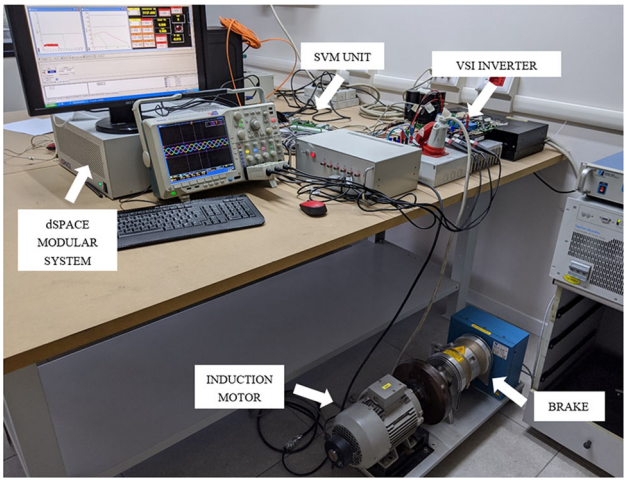

Fig. 22 Test bench setup

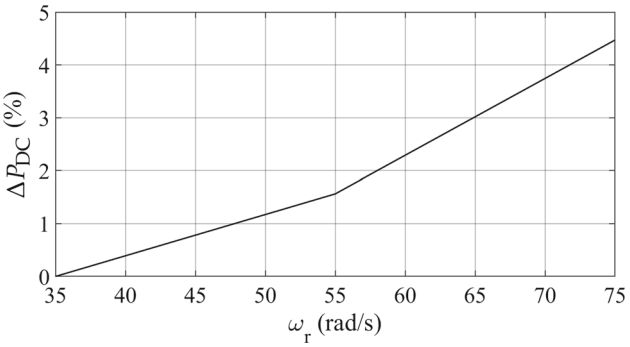

Fig. 23 Experimental results: reduction of the DC power ΔP_{DC} delivered from the power supply to the VSI DC link, which is achieved by means of the MTPW control strategy with respect to the MTPA one, for $T^* = 3.5$ Nm

and DS2004 boards have been used, respectively, to acquire the digital signals from the speed sensor and the analog ones from current and voltage sensors. In order to validate the numerical analysis, experimental tests have been performed considering steady state operating points of the first part of the numerical analysis with a load torque T_L equal to 3.5 Nm, which is applied to the motor shaft at different values of the ω_r by means of a dynamic controllable brake (Fig. (22)). In detail, Fig. (23) shows the reduction of the DC power, ΔP_{DC}, delivered from the power supply to the VSI DC-link, which has been achieved using the proposed MTPW instead of MTPA control strategy. The introduction of the quantity ΔP_{DC} indirectly allows evaluating the reduction of the total power losses that is achievable with the proposed control algorithm solution. In detail, considering as experimental mechanical speed range one of Fig. (18) of the numeric analysis, it is possible to notice how the MTPW control strategy allows performing a reduction of the ΔP_{DC}, which is fully comparable with the reduction losses reported in Fig. (18). Figures (24) and (25), respectively, report the waveform of

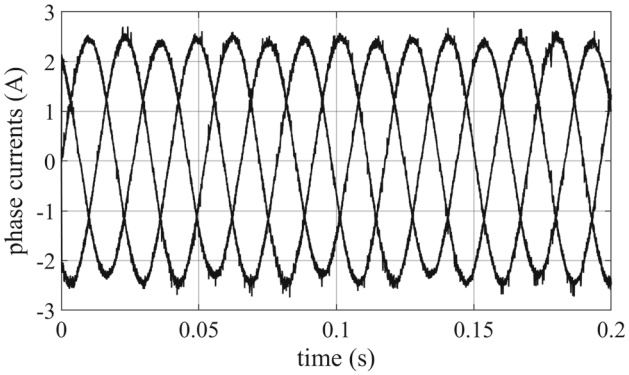

Fig. 24 Experimental results: phase currents when MTPA control is adopted (peak value 2.33 A) with $T^* = 3.5$ Nm and ω_r =75 rad/s

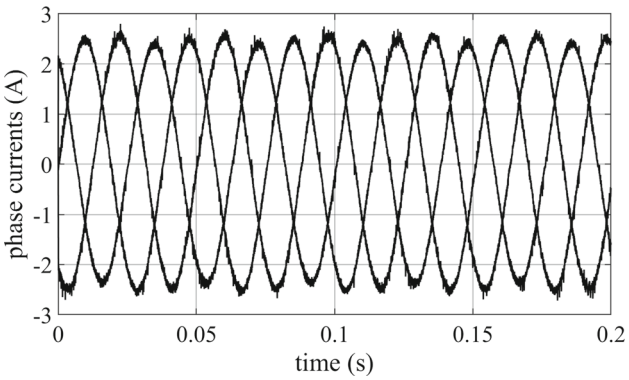

Fig. 25 Experimental results: phase currents when MTPW control is adopted (peak value 2.42 A) with $T^* = 3.5$ Nm and ω_r =75 rad/s

motor phase currents for MTPA and MTPW control strategies when ω_r=75 rad/s. Even if the amplitude of the MTPW currents (2.42 A) is higher than the one of the MTPA currents (2.33 A), the proposed control strategy allows reducing the needed power to fed the electric drive with the minimization of its total power losses. This confirms the validity of the proposed theoretical approach and of the numerical analysis as well.

6 Conclusion

A new field-oriented control strategy for induction motor has been presented. It is called Maximum Torque Per Watt (MTPW) and allows achieving the minimum value of the sum of the stator and rotor losses due to joule effect, and of the iron losses, for a given value of the reference torque and of the motor speed. Iron losses have been modeled according to Steinmetz equation, separating hysteresis and eddy currents and taking into account the dependence both on the frequency and on the peak value of the flux density. Numerical and experimental results have confirmed the validity of the proposed approach, which allows obtaining signifi-

cant performance improvements of induction motor drives in terms of the efficiency increments especially at light load operating conditions.

Funding Open access funding provided by Università degli Studi di Napoli Federico II within the CRUI-CARE Agreement.

Compliance with ethical standards

Conflicts of interest The authors declare that they have no conflict of interest.

References

1. Leonhard W (1985) Control of electrical drives. Springer, Berlin
2. Bose BK (1986) Power electronics and AC drives. Prentice-Hall, Englewood Cliffs, New Jersey
3. Kirschen DS, Novotny DW, and Suwanwisoot W (1984) "Minimizing Induction Motor Losses by Excitation Control in Variable Frequency Drives". In: IEEE Transactions on Industry Applications IA-20.5, pp. 1244-1250
4. Sul SK, Park MH (1988) A novel technique for optimal efficiency control of a current-source inverter-fed induction motor. IEEE Trans Power Electr 3(2):192–199
5. Famouri P, Cathey JJ (1991) Loss minimization control of an induction motor drive. IEEE Trans Ind Appl 27(1):32–37
6. Wasynczuk O et al (1998) A maximum torque per ampere control strategy for induction motor drives. IEEE Trans Energy Convers 13(2):163–169
7. Geng H, Yang G, Mu C (2005) "A Novel Torque Control Strategy of Induction Motors Taking Efficiency of Dynamic State into Account". In: 2005 IEEE 36th Power Electronics Specialists Conference. pp 694-700
8. Huihui X et al. (2016) "A novel MTPA control strategy of induction motor based on torque current compensation". In: 2016 19th International Conference on Electrical Machines and Systems (ICEMS). pp 1-4
9. Jae Ho Chang and Byung Kook Kim (1997) Minimum-Time minimum-loss speed control of induction motors under field-oriented control. IEEE Trans Ind Electr 44(6):809–815
10. Lorenz RD, Yang SM (1992) Efficiency-optimized flux trajectories for closed-cycle operation of field orientation induction machine drives. IEEE Trans Ind Appl 28(3):574–580
11. Sangwongwanich S et al (1991) Realization of time-optimal single-step velocity response control of field-oriented induction machines under the condition of nonsaturation of flux. IEEE Trans Ind Electr 27(5):947–955
12. Gonzalez CMV, Arribas JR, Prieto DR (2006) Optimal regulation of electric drives with constant load torque. IEEE Trans Ind Electr 53(6):1762–1769
13. Botan C, Ratoi M, and Horga V. (2008) "Optimal control of electrical drives with induction motors for variable torques". In: Proceedings of 13th International Power Electronics Motion Control Conference. IEEE, pp 1111-1116
14. de Wit CC, Ramirez J (1999) Optimal torque control for current-fed induction motors. IEEE Trans Autom Control 44(5):1084–1089
15. Stumper JF, Dotlinger A, Kennel R (2013) Loss minimization of induction machines in dynamic operation. IEEE Trans Energy Convers 28(3):726–735
16. Attaianese C et al (2020) A variational approach to MTPA control of induction motor for EVs range optimization. Trans Veh Technol 69(7):7014–7025
17. Kioskeridis I, Margaris N (1996) Loss minimization in induction motor adjustable-speed drives. IEEE Trans Ind Electr 43(1):226–231
18. Uddin MN, Nam SW (2008) New online loss minimization-based control of an induction motor drive. IEEE Trans Power Electr 23(2):926–933
19. Krings A et al. (2012) "Measurement and Modeling of Iron Losses in Electrical Machines". In: 5th International Conference Magnetism and Metallurgy WMM
20. Steinmetz CP (1892) "On the Law of Hysteresis". In: Transactions of the American Institute of Electrical Engineers IX.1, pp 1-64
21. Jordan H. (1924) "Die ferromagnetischen Konstanten für schwache Wechselfelder". In: Elektrische Nachrichten Technik 1
22. Burais N (1981) "Iron Losses Calculation in Non-Oriented Steel Plate". In: IEEE Transactions on Magnetics 17.6
23. Pfützner H et al. (1991) "Problems of loss separation for crystalline and consolidated amorphous soft magnetic materials". In: IEEE Transactions on Magnetics 27.3
24. Boglietti A et al. (1998) "Loss Separation Analysis in Ferromagnetic Sheets under PWM Supply". In: IEEE Transactions on Magnetics 34.4
25. Boglietti A, Lazzari M. and Pastorelli M (1997) "Iron Losses Prediction with PWM Inverter Supply using Steel Producer Data Sheet". In: Proceedings of IEEE Industry Application Society Annual Meeting
26. Li J, Abdallah T, Sullivan C (2001) "Improved calculation of core loss with nonsinusoidal waveforms". In: Conference Records of 36th IAS Annual Meeting. vol 4, pp 2203-2210
27. Attaianese C, Di Monaco M, Tomasso G (2010) "High Performance Power Converter for Combined Batteries-Supercapacitor Systems". In: Proceedings of XIX International Conference on Electrical Machines (ICEM), pp. 1-6